

Crystal chemistry and Mössbauer spectroscopic analysis of clays around Riyadh for brick industry

Mutasim I. Khalil

Published online: 31 January 2013
© Springer Science+Business Media Dordrecht 2013

Abstract A total of 30 clay samples were collected from the area around Riyadh city, Saudi Arabia. A complete chemical analysis was carried out using different techniques. X-ray diffraction studies showed that the clay samples were mainly of the smectite group with traces of the kaolinite one. The samples studied were classified as nontronite clay minerals. One of the clay fraction has been studied by Mössbauer spectroscopy as raw clay fraction and after being fired at 950–1,000 °C. The Mössbauer spectra showed accessory iron compounds in the form of hematite and goethite. The structural iron contents disintegrate on firing transforming into magnetic iron oxide and a paramagnetic small particles iron oxide.

Keywords Clay bricks · Iron oxides · Smectite · Nontronite · Montmorillonite · Mössbauer spectroscopy

1 Introduction

Clay minerals, in general, are fine grained, hydrous, aluminium silicates with laminar structure made of octahedral and tetrahedral sheets as building blocks. These are arranged in a special arrangement depending on the type of clay mineral [1, 2]. Their physical properties and chemical compositions are determined by the geological conditions in which they were formed [3].

The present investigation aims to throw light on the nature, classification and economical application of clays around Riyadh. For that purpose, crystal structure was investigated using different techniques. The classification scheme for phyllosilicates

International Symposium on the Industrial Applications of the Mössbauer Effect (ISIAME 2012), Dalian, China, 2–7 September 2012.

M. I. Khalil (✉)
Department of Chemistry, College of Science, King Saud University,
P.O. Box # 2455, Riyadh 11451, Saudi Arabia
e-mail: mkhalil@ksu.edu.sa

used here is the one agreed upon by mineralogists throughout the world, i.e. the phyllosilicates are divided into groups each containing di- and tri-octahedral groups each containing di- and tri-octahedral subgroups. The later is in turn divided into mineral species [4].

The Mössbauer effect proved to be an excellent method for studying iron cation positions in layer silicate minerals and has been used to establish the presence of Fe^{2+} and Fe^{3+} in clay minerals [5]. The isomer shift observed in the Mössbauer spectrum indicates the valence state of the iron in the clay mineral. The magnitude of the quadrupole splitting reflects the local surroundings of the iron ions. In sheet structure silicates, octahedrally coordinated iron can be distinguished from the tetrahedral iron. Siderite and goethite, common contaminants of the clay minerals, can usually be detected by the help of Mössbauer spectroscopy [6–8]. However, the various families of clay minerals show minor differences in isomer shift and quadrupole splitting caused by variation in the character at the octahedral layer [5].

Fired clays, which undergo changes in their structural iron contents, have been studied by Mössbauer spectroscopy, e.g. changes in the spectra of Fe in biotite are observed in samples heated in air at 700 °C [6]. Heat treatment of mica samples at 100 °C yield magnetic hyperfine patterns [7]. Pottery clay fired at 1,200 °C was also studied where upon decrease in magnetic field was observed [8].

We here report crystal chemistry, classification and Mössbauer analyses of some raw and fired Saudi clay for the benefit of clay bricks industry.

2 Experimental

2.1 Sampling

The area around Riyadh (Saudi Arabia) was chosen on merit of geographic and economical importance. Thirty samples were collected from different depths and sites.

2.2 Analysis

Samples were sieved in a 60 mesh so as to enhance fusion and reduce matrix in XRF analysis. X-ray diffraction studies were performed using a Sintage high resolution computerized powder X-ray diffractometer with a Si-Li detector. Oriented samples were prepared by transferring a filtered clay suspension through a 0.45 micron pore-size filter to a glass microscope slide. Measurements in the 3–60° 2 θ region were performed on the samples without treatment and another measurement was done on sample A and B after being left in a desiccator with ethylene glycol at 60 °C over night. The d-spacings for the different reflections and their net intensities were obtained using on-line computer with subroutines for background subtraction and peak search finder.

Absorbed and crystal H_2O were determined at 110 °C and 1,000 °C, respectively, using a silica crucible and the presence of carbonate was checked by HCl treatment.

SiO_2 was determined colourimetrically using standard albite, while Al_2O_3 was determined volumetrically by EDTA in the presence of Fe and Ti. The albite

Table 1 Typical chemical assay of clay samples wt%

Sample number	1	2	3	4	5	6	7
SiO ₂	49.2	55.1	55.5	45.9	54.8	58.2	45.2
TiO ₂	0.76	2.76	0.63	1.47	1.94	2.60	1.14
Al ₂ O ₃	12.6	13.8	13.5	14.9	12.4	10.1	11.0
Fe ₂ O ₃	8.7	9.68	10.5	19.4	10.2	9.68	7.2
CaO	7.88	1.87	1.21	1.34	2.19	2.79	9.24
MgO	2.22	1.90	1.65	0.36	1.89	1.94	2.42
Na ₂ O	0.90	2.47	1.04	0.33	1.60	1.96	0.41
K ₂ O	1.04	1.25	1.19	0.47	1.09	1.20	0.67
H ₂ O(adsorbed)	6.17	4.30	6.64	2.24	4.81	4.82	7.64
H ₂ O(crystal)	10.3	6.76	7.94	12.5	9.01	6.12	14.4
Total	99.8	99.8	99.7	99.9	99.9	99.4	99.9

Table 2 Combined Fe₂O₃ determined colourimetrically after Iron oxide removal

Sample no.	Wt.% of Fe ₂ O ₃
1	8.44
2	9.60
3	8.52
4	2.57
5	3.63
6	9.29
7	7.75

standard used contains 18.61 % Al₂O₃, Fe₂O₃, CaO, MgO, Na₂O and K₂O were determined by flame photometry in an oxine medium.

TiO₂, Fe₂O₃ and CaO were also determined by XRF. The matrix variations, particle size and surface finish effects were reduced by sieving the sample in a 60 mesh. Cd was used as a source with Si-Li detector, and time of collection was 500 sec. Analytical results are shown in Table 1.

Trace elements were qualitatively determined by XRF and found to be Li, P, S, Cl, Mn, Ni, Cu, Zn, Br, Sr, Rb, Zr, Y and Nb.

2.3 Removal of accessory iron compounds

The clay samples were treated by Jackson method [9] to prepare 2 μ particle size samples and then the accessory iron oxides were removed by adding 40 cm³ of 0.3 M Na-citrate solution and 5 cm³ of 1 M NaHCO₃ solution to 10 g of clay sample. The temperature was brought to 80 °C using a sand bath, then 1 g of Na₂SO₄ was added. The mixture was stirred for one minute and then occasionally for a total of 15 min. 10 cm³ of saturated NaCl solution was then added and the mixture was centrifuged for 5 min. at 1,600–2,200 rpm. This treatment was repeated once more and the sample was washed three times with deionized water and dried at room temperature. The combined Fe₂O₃ in these samples were then calorimetrically determined, Table 2. The above treated samples (2 μ) and the untreated ones (60 μ) were both fired at 950–1,000 °C for 3 h and their Mössbauer spectra were then recorded by taking 0.15 g of the sample mixed with 0.07 g of charcoal using diethyl ether and placed in a copper ring using aluminum foil. A ⁵⁷Co-Rh source was used and the low temperature measurements were done using liquid nitrogen (80 K) with

Table 3 Chemical formula of the selected clay samples

Sample no.	Structural formula								
1	(Ca ²⁺ , K ¹⁺ , Na ¹⁺)			(Al ³⁺ , Fe ³⁺ , Mg ²⁺)			(Si ⁴⁺ , Al ³⁺) O ₂₀ (OH) ₄		
	1.3	0.20	0.27	1.82	0.97	0.51	7.54	0.45	
2	(Ca ²⁺ , K ¹⁺ , Na ¹⁺)			(Al ³⁺ , Fe ³⁺ , Fe ²⁺ , Mg ²⁺)			(Si ⁴⁺ , Al ³⁺) O ₂₀ (OH) ₄		
	0.15	0.12	0.69	2.35	0.92	0.14	0.41	7.99	0.01
3	(Ca ²⁺ , K ¹⁺ , Na ¹⁺)			(Al ³⁺ , Fe ²⁺ , Mg ²⁺)			(Si ⁴⁺ , Al ³⁺) O ₂₀ (OH) ₄		
	0.19	0.22	0.30	2.34	0.94	0.36		8.00	0.00
4	(Ca ²⁺ , K ¹⁺ , Na ¹⁺)			(Al ³⁺ , Fe ³⁺ , Mg ²⁺)			(Si ⁴⁺ , Al ³⁺) O ₂₀ (OH) ₄		
	0.26	0.11	0.13	3.08	0.46	0.23		8.00	0.00
5	(Ca ²⁺ , K ¹⁺ , Na ¹⁺)			(Al ³⁺ , Fe ³⁺ , Fe ²⁺ , Mg ²⁺)			(Si ⁴⁺ , Al ³⁺) O ₂₀ (OH) ₄		
	0.35	0.46	0.46	2.15	0.94	0.10	0.42	8.00	0.00
6	(Ca ²⁺ , K ¹⁺ , Na ¹⁺)			(Al ³⁺ , Fe ³⁺ , Fe ²⁺ , Mg ²⁺)			(Si ⁴⁺ , Al ³⁺) O ₂₀ (OH) ₄		
	0.43	0.22	0.54	1.71	0.88	0.13	0.42	8.00	0.00
7	(Ca ²⁺ , K ¹⁺ , Na ¹⁺)			(Al ³⁺ , Fe ³⁺ , Fe ²⁺ , Mg ²⁺)			(Si ⁴⁺ , Al ³⁺) O ₂₀ (OH) ₄		
	1.64	0.14	0.13	1.65	0.85	0.12	0.60	7.51	0.49

the help of a continuous flow cryostat in conjunction with a temperature controller. The Mössbauer spectra of the selected samples prepared at different conditions are shown in Fig. 2. The corresponding Mössbauer parameters are presented in Table 4. The data were calibrated using α -iron at room temperature.

3 Results and discussion

3.1 Chemical formula: [(Na,K,Ca)_{0.5–1.91}(Fe³⁺, Al, Fe²⁺, Mg)_{3.14–3.82}(Si_{7.51–8.0}Al_{0.0–0.49})O₂₀(OH)₄

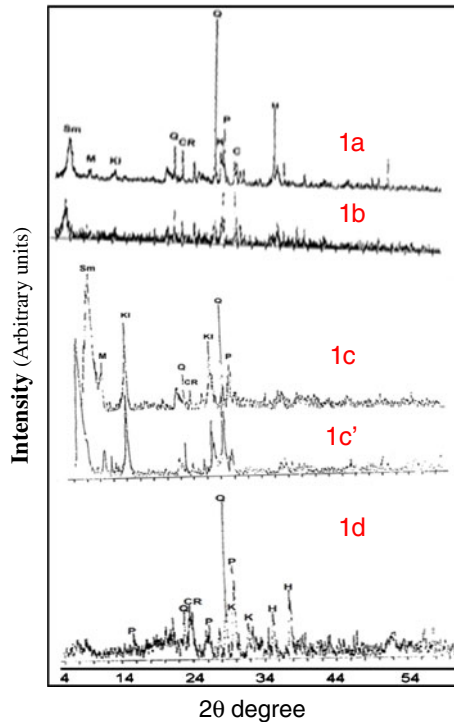
Table 1 represents the elemental composition of samples. The indicated composition is typical of these clays. These data can be explained by the similar origin of the clays which were found under the same conditions of climate. Only seven samples were chosen for comparative studies and their structural formulas were derived. Titanium is not considered as part of the clay structure since its presence is attributed to anatase or rutile [10].

The calculations were based on a unit cell consisting of 44 negative charges, i.e. O₂₀, (OH)₄ see Table 3.

3.2 XRD spectra

Figure 1a and b shows the X-ray diffraction pattern taken for sample A before and after ethylene glycol treatment. The expansion of the ~ 14 Å reflection peak to ~ 17 Å confirms that the smectite group is constituent of these clays. The diffraction pattern also shows that kaolinites (only traces were detected), cristobalite, calcite and mica are present, but the dominant constituents are quartz and feldspars. The XRD patterns of sample B, Fig. 1c, shows that the smectite and kaolinite are very much enhanced. The removal of accessory iron oxides greatly enhanced the parallel orientations of the layered silicates and clearly changed the relative abundance of

Fig. 1 *1a* before and *1b* after ethylene glycol treatment of raw clay; *1c* before and *1c'* after ethylene glycol treatment of the clay sample freed from accessory iron; *1d* fired sample. *Sm* smectite; *KI* kaolinite; *Q* quartz; *P* plagioclase; *M* mica; *CR* cristobalite



the different minerals. The clay fraction also consists of quartz, feldspars, mica and cristobalite. Calcite seems to have been washed out with the accessory iron oxide. The analysis of the fired samples has shown that quartz, feldspars, cristobalite and haematite are present Fig. 1d.

For the fired samples it is clear that the core of the diffraction pattern became larger than that before firing. This means there was an expansion of the lattice due to firing.

3.3 Mössbauer spectra

The structure of the observed Mössbauer spectrum, Fig. 2(left(A) and right(A)), consists of a six line pattern arising from magnetic hyperfine splitting in magnetically ordered compound and a central doublet pattern due to quadrupole splitting. The hyperfine splitting is completely absent in the spectrum of the clay sample freed from accessory iron components, Fig. 2(left(B) and right(B)). From the values of hyperfine parameters, Table 4, this accessory iron oxide is believed to be either hematite ($\alpha\text{-Fe}_2\text{O}_3$) or goethite ($\alpha\text{-FeOOH}$) [11]. Raw, i.e., unfired clays, contain iron in the clay fraction in varying amounts of accessory iron oxides and hydroxides [12]. Due to its high thermodynamic stability, goethite is the most common Fe oxide in soils and is commonly associated with hematite in warm regions [13]. Hence, the six line ^{57}Fe Mössbauer spectrum, Figs. 2(left(A) and right(A)), of clay in as received state could be tentatively assigned to either hematite or goethite [2, 14] or both. Pure hematite Mössbauer spectrum shows a large hyperfine splitting with a hyperfine

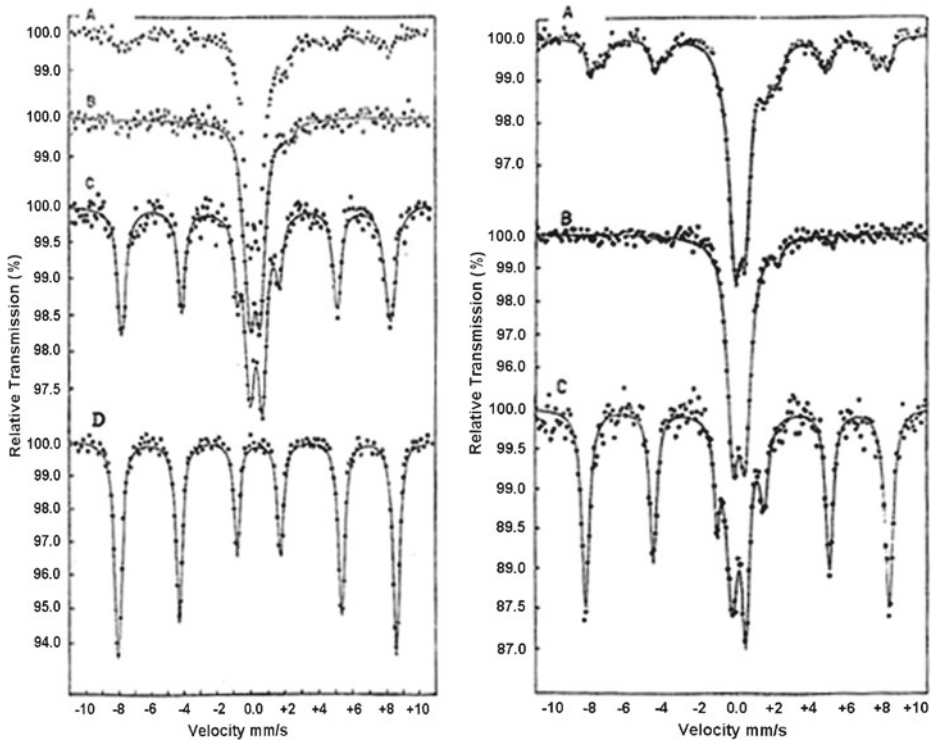


Fig. 2 Room temperature (*left*) and 80 K (*right*) ^{57}Fe Mössbauer spectra of a clay sample originated around Riyadh (*A*) in as received state, (*B*) after separating Fe_2O_3 from the sample, (*C*) after firing the sample from which Fe_2O_3 was separated and (*D*) of standard $\alpha\text{-Fe}_2\text{O}_3$

field of about 52 T at 300 K in agreement with values observed, Table 4. On the other hand, well crystallized goethite orders antiferromagnetically at 400 K and one observes a magnetic hyperfine splitting at RT with a hyperfine field of 38 T and a quadrupole interaction of -0.26 mm/s [15–17]. This 38 T component is absent in the 300 K, Table 4, spectrum ruling out the presence of goethite. The concentration of the accessory iron oxides contents determined chemically for two samples were; 0.80 and 0.9 % compared to 0.97 and 0.86 % determined by Mössbauer spectroscopy, Table 2. The central doublet is assigned to structural iron in octahedral sites. The intense doublet in Fe^{3+} state observed by Tripathi et al. [1] in the Mössbauer spectrum of a China clay sample was assigned to iron in cis site of the clay mineral, while the faint sextet was assigned to hematite. The range of the isomer shift between 0.3 and 0.5 mm/s and a quadrupole splitting Δ , between -0.6 and -0.76 mm/s are typical values for octahedral ferric ions as suggested by Coey [18]. He reported that the typical parameters for ferric ions in tetrahedral positions are 0.17 mm/s for isomer shifts and 0.5 mm/s for quadrupole splitting. Weaver [5] found that in nontronite Fe^{3+} octahedron exhibits an isomer shift of 0.3 mm/s and a quadrupole splitting of ≈ 0.3 mm/s and in montmorillonite it exhibits an isomer shift of ≈ 0.4 mm/s. Eleven samples of montmorillonite and nontronite studied by Coey [18] exhibited mean isomer shifts and quadrupole splitting values of ≈ 0.38 and ≈ 0.5 mm/s, respectively.

Table 4 Mössbauer parameters of: (A) as received, (B) iron oxide removed, (C) fired clay samples

Sample	TK	Site (%)	δ (mm/s)	Δ (mm/s)	$B_{\text{hf}}T$	W (mm/s)
A	80	Fe ³⁺ (53)	0.43	-0.60	-	0.60
		Fe ²⁺ (16)	1.12	-2.70	-	0.60
		M1(14)	0.54	-0.27	49.6	0.54
		M2(17)	0.50	-0.18	52.0	0.54
	300	Fe ³⁺ (87)	0.35	-0.59	-	0.27
		Fe ²⁺ (13)	1.09	-1.79	-	0.62
B	80	Fe ³⁺ (92)	0.42	0.67	-	0.60
		Fe ²⁺ (08)	1.14	2.79	-	0.50
	300	Fe ³⁺ (91)	0.32	0.59	-	0.69
		Fe ²⁺ (09)	1.03	2.67	-	0.50
C	80	Fe ³⁺ (36)	0.44	-0.76	-	0.65
		M2 (64)	0.44	-0.27	52.7	0.48
	300	Fe ³⁺ (40)	0.34	-0.74	-	0.66
		M2(60)	0.39	-0.31	49.6	0.52
α -Fe ₂ O ₃	300	M2(100)	0.37	-0.29	51.4	0.44

M1 and M2 denote the goethite hematite iron site respectively

Erricson [19] concluded that typical parameters show large overlap from one species to another. Taylor et al. [20] reported that the Mössbauer spectrum of nontronite shows a single peak, actually an unresolved doublet, corresponding to ferric iron in a single site. Iron in nontronite usually occurs in the octahedral layer [21].

In the region of firing temperature between 950 and 1,000 °C changes in the structure of the central paramagnetic part is observed which is attributed to transformations in the clay mineral structure. The results of Fig. 2(left(C)) shows appearance of a magnetic component upon firing which is associated with the dehydroxylation of the clay minerals and transformation into hematite. The paramagnetic part is persistent in the spectrum indicating that this component is due to a magnetically ordered species in the form of fine particles [14, 22]. The relative decrease in the paramagnetic component and appearance of a relatively large area of the magnetic component suggest that at this firing temperature iron diffuses out of the lattice and appears as a magnetic oxide, i.e., α -Fe₂O₃, in accord with the XRD results. The significant enhancement of the magnetic part between the Mössbauer spectrum of the unfired clay and the spectrum of the fired clay implies an apparent increase in particle size of the oxide component of the clay. The size was estimated to be doubled at 900 °C [14]. The Mössbauer of hematite particles smaller than 10 nm is a quadrupole doublet only [22, 23]. The lower the temperature becomes, the more the particles become blocked and exhibit a magnetic hyperfine structure. The spectra then consist of a superposition of a magnetically split sextet arising from the blocked particles and a quadrupole doublet arising from those in the limit of fast supermagnetic relaxation [24], as observed in Fig. 2. Although the clay sample under study is non-calcareous, but depending on the particle size and distribution of the Ca-bearing carbonate in the clay matrix, one might expect the formation of calcium silicate phases, e.g., gehlenite, Ca₂Al [(Si, Al)₂O₇], that tends to form above

about 900 °C in calcareous clays [25]. This will then contribute to the paramagnetic Mössbauer pattern of the fired sample, Fig. 2(left(C) and right(C)), observed [25, 26].

4 Conclusion

In this paper we present the results of chemical analysis, XRD, XRF and Mössbauer spectral studies performed on 30 clay samples collected from Riyadh area in Saudi Arabia. The results are indicative of the fact that the dominant clay mineral group is the smectite one. With high iron content found, these smectite minerals belong to nontronite, which is the iron rich end members of the smectite group, rather than to montmorillonite [14, 27].

The results presented in this paper demonstrate that Mössbauer spectroscopy can provide a detailed description of the iron containing phases in a clay and of the transformations that occur during firing. At $\approx 1,000$ °C the structural iron component has formed a magnetic phase during disintegration of the clay mineral structure. The appearance of the paramagnetic component in the spectrum is attributed to fine iron oxide particles formed not ruling out the formation of calcium silicate phases. Finally, firing Riyadh clay minerals at 1,000 °C will ensure a deep red colour favoured by the manufacturers of clay bricks. It remains to investigate the effect of oxidizing and reducing conditions on the colour of bricks manufactured from such local clays.

Acknowledgement This project was supported by King Saud University, Deanship of Scientific Research, College of Science, Research Center.

References

1. Tripathi, R.P., Verma, H.C., Chandrasekhar, S., Ramaswamy, S., Gajbhiye, N.S., Date, S.K.: ICAME (2007). doi:10.1007/978-3-540-78696-2_142
2. Huaypar, Y., Bravo, J., Gutarra, A., Gabriel, E.: *Hyperfine Interact.* **175**, 23–28 (2007). doi:10.1007/s10751-008-9583-2
3. Moore, D.M., Reynolds, R.C. Jr.: *X-Ray Diffraction and the Identification and Analysis of Clay Minerals*, 2nd edn. Oxford University Press, Oxford (1997)
4. Bailey, S.W., Barindley, G.W., Kodam, H., Martin, R.T.: *Clays Clay Miner.* **30**(1), 76–78 (1982)
5. Charles, E.W., Wampler, J.M., Pecuil, T.E.: *Science* **19**, 504–508 (1967)
6. Amirahanov, Kh.L., Anokhina, L.K., Sardarov, S.S.: *CA* **91**, 213910 n (1979)
7. Tripathi, R.P., Chandra, V., Chandra, R., Lokanathan, S.: *J. Inorg. Nucl. Chem.* **40**(7), 1293–1298 (1978)
8. Chevalier, R., Coey, J.M.D., Bouchez, N.: *J. Phys. Colloq.* **9**, 861–865 (1976)
9. Jackson, M.L.: *Soil Chemical Analysis Advanced Course*, pp. 45–47. USA (1956)
10. Grim, R.E.: *Clay Mineralogy*, 2nd edn. McGraw Hill Book Co. (1968)
11. Murad, E.: *Phys. Chem. Miner.* **23**, 248–262 (1996)
12. Murad, E., Wagner, U.: *Hyperfine Interact.* **45**, 161–177 (1989)
13. Cornwell, R.M., Schwertmann, U.: *Soils*, 2nd edn. In: WILEY-VCH (ed.) *The Iron Oxides; Structure, Properties, Occurrences and Uses*, pp. 441–442 (2000)
14. Simopoulos, A., Kostikas, A., Singlas, I., Gangad, N.H., Moukarika, A.: *Clays Clay Miner.* **23**(5), 393–399 (1975)
15. Murad, E., Cashion, J.: *Mössbauer Spectroscopy of Environmental Materials and their Industrial Utilization*. Kluwer, Boston (2003)
16. Keisch, B.: *Nucl. Instrum. Methods* **104**, 237–240 (1972)
17. Murad, E., Johnston, J.H.: *Iron oxides and oxyhydroxides*. In: Long, G.J. (ed.) *Mössbauer Applied to Inorganic Chemistry*, vol. 2, pp. 507–582. Plenum, New York (1987)
18. Coey, J.M.D.: *At. Energy Rev.* **181**, 73–124 (1980)

19. Ericsson, T., Linares, L., Lotse, E.: *Clay Miner.* **19**(1), 85–91 (1984)
20. Taylor, G.L., Routsala, A.P., Keeling, R.O. Jr.: *Clays Clay Miner.* **16**, 381–391 (1968)
21. Grim, R.E.: *Clay Mineralogy*. McGraw-Hill, New York (1953)
22. Gangas, N.H., Simopolous, A., Kostikas, K., Yassoglu, N.J., Filippakis, S.: *Clays Clay Miner.* **21**, 151–160 (1973)
23. Kundig, W., Bommel, H., Constabaris, G., Lindroos, R.H.: *Phys. Rev.* **142**, 327–333 (1966)
24. Wagner, F.E., Wagner, U.: *Hyperfine Interact.* **154**, 35–82 (2004)
25. El-Hage, Y., Wagner, U., Wagner, F.E., Riederer, J., Echt, R., Hachmann, R.: *Hyperfine Interact.* **57**, 2173–2178 (1990)
26. Maniatis, Y., Simopoulos, A., Kostikas, A.: *J. Am. Ceram. Soc.* **64**, 263–269 (1981)
27. Oyawoye, M.O., Krist, D.M.: *Clay Miner. Bull.* **5**, 527–533 (1964)